Optik xxx (2013) xxx–xxx

Contents lists available at SciVerse ScienceDirect

Optik

journal homepage: www.elsevier.de/ijleo

Design and analysis of nano-deep corrugated waveguide grating-based dual-resonant filters in visible and infra-red regions

Mukesh Sharma, Suchandan Pal*

Optoelectronic Devices Group, Council of Scientific and Industrial Research – Central Electronics Engineering Research Institute (CSIR-CEERI), Pilani, Rajasthan 333 031, India

ARTICLE INFO

Article history:
Received 6 June 2012
Accepted 30 October 2012

Keywords:
Long-period waveguide grating (LPWG)
NOA61 optical epoxy
Optical waveguide filters
Polymer waveguides
SU-8 polymer

ABSTRACT

A theoretical analysis of nano-deep corrugated long-period waveguide gratings on a SU-8 polymer-based channel waveguide with NOA61 optical epoxy coated upper- and lower cladding is presented. The transmission spectra of the gratings show strong rejection bands both at visible (at wavelength region of 450–460 nm) and infra-red (at wavelength region of 1530–1540 nm) regions when a grating period of ~68 μm with optimized grating tooth height is considered. Phase-matching graphs are studied to find the relationship between resonance wavelength and grating period. These results show that the grating parameters significantly affect the characteristics of transmission spectra as well as the resonance wavelength of the grating. Long-period waveguide grating-based band pass filter made by use of same polymer materials are also designed and analyzed. These types of waveguide grating-based filters can widely be used for visible and infra-red wavelength sensing applications.

1. Introduction

Long-period waveguide grating (LPWG)-based devices have attracted considerable interest in recent years in the field of optical communication and sensor applications because of the flexibility in their structures and materials as compared to the long-period fiber gratings [1]. The use of optical fiber-based grating devices is generally inappropriate when integration is required; planar light wave technology is advantageous in this respect. Also, waveguide-based gratings [2] are superior to fiber-based devices in case of ease in mass production. The flexibility of the optical waveguide technology allows long-period gratings to be fabricated in different waveguide structures with different materials. Polymer LPWG-based devices [3,4] are attractive because of its small size, low cost, simple process, and potential integration with other components on the same substrate. Further, polymer materials are photosensitive; therefore, polymer-based LPWGs have been found to be popular in various sensing applications because of their high sensitivity and wide-range tuning capability due to the relatively high thermo optic coefficient value of polymers. Polymers offer excellent potential for the realization of low cost WDM components because they can be fabricated easily at low temperature on various kinds of substrates. In particular, the large thermooptic (TO) coefficient of polymer makes possible the realization of efficient thermally tunable devices, such as band-rejection filter, band pass filter [5], variable-tunable filter [6–8], and grating couplers [9,10]. Researchers have also reported the dual-resonance LPWGs [11], based on polymer materials having their two distinct resonance wavelengths very close to each other in the wavelength region of 1500 nm. This device can effectively be used for temperature compensated sensing applications but with a limited dynamic range. In this paper, NOA-61 and SU-8 polymer-based dual resonance LPWG has been proposed for which one of the resonance wavelengths appear in the visible region (450–460 nm) while the other resonance wavelength in the infra-red region (1530–1540 nm). The device can be used for sensing applications having a much wider dynamic range. Further, it can also be utilized for visible and infra-red sensing applications simultaneously or separately.

In this paper, the design and theoretical analysis of nano-deep corrugated polymer LPWG-based devices like band-reject and band-pass filters are presented. SU-8 2005 polymer is considered as the waveguide material and Norland Optical Adhesive 61 (NOA 61) optical epoxy has been proposed for under- and over-cladding of the device. MicroChem Nano™ SU-8 2000 series polymer is a negative tone photoresist polymer, which has been considered as the guiding layer of the LPWG. This polymer has considerably high optical transparency above 360 nm wavelength. Cured SU-8 is highly resistant to solvents, acids and bases, and has excellent thermal stability making it well suitable for applications in which cured materials are permanent structures of the device. On other side, NOA 61 is a clear, colorless, liquid UV-curable photopolymer. The refractive indices of SU-8 2005 and cured NOA 61 are considered 1.57, 1.55, respectively, at 1550 nm wavelength as per their measurements reported [12].

* Corresponding author. Tel.: +91 1596 252286; fax: +91 1596 242294.
E-mail address: spal@ceeri.ernet.in (S. Pal).

0030-4026/$ – see front matter © 2012 Elsevier GmbH. All rights reserved.
http://dx.doi.org/10.1016/j.ijleo.2012.10.066

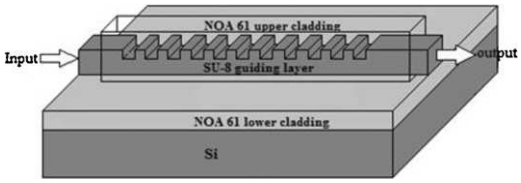

Fig. 1. Schematic of a nano-deep corrugated polymer LPWG structure for band reject filter.

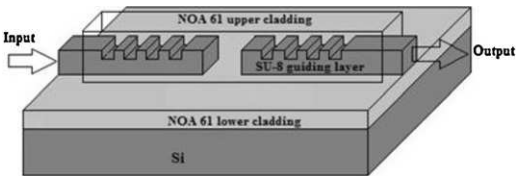

Fig. 2. Schematic of an LPWG structure for band pass filter.

The LPWG device is so designed that its transmission spectra show strong rejection bands in visible as well as infra-red (IR) wavelength regions. The transmission spectra of the LPWGs and the phase-matching graphs for transverse electric (TE) and transverse magnetic (TM) polarizations have been studied. The variation of the grating spectral characteristics has been investigated with the variation of the waveguide and the grating parameters like the period of the grating, tooth height of the grating corrugation. Subsequently, LPWG-based band-pass filter has also been designed

2. Basic theory of LPWG

A long-period waveguide grating (LPWG)-based device consists of a higher indexed partially corrugated guiding layer with relatively lower indexed under-cladding and over-cladding layers. The corrugated grating is capable of coupling light from the fundamental core mode to selected cladding modes at specific wavelengths (known as the resonance wavelengths) and thus gives rise to a number of rejection bands in the transmission spectrum. Based on the coupled-mode theory [13], grating period, Λ, and resonance wavelength of the LPWG, λ_0, are related by a phase matching condition,

$$\lambda_0 = (N_0 - N_m)\Lambda \quad (1)$$

where N_0 and N_m ($m = 1, 2, 3, \ldots$) are mode indices of forward propagating fundamental core-mode and that of the higher order cladding modes propagating in the same direction, respectively. The rejection-band isolation strength of the LPWG is primarily determined by the coupling coefficient of the device, which is governed by the overlap of three spatial distributions: (i) the transverse field distribution of the fundamental core-mode in the waveguide, ψ_0 (x, y), (ii) the transverse field distribution of different higher order cladding modes, ψ_m (x, y), and (iii) the transverse distribution of the refractive-index modulation of the grating, Δn (x, y). Therefore, the coupling coefficient equation may be expressed as

$$\kappa_{0m} \propto \int\int \Psi_{*0}(x,y)\Psi_m(x,y)\Delta n(x,y)\mathrm{d}x\,\mathrm{d}y \quad (2)$$

where ψ^*_0 (x, y) is the complex conjugate of the transverse field distribution of the fundamental core-mode [14]. The spatial distributions of these three functions depend on the spatial characteristics of the waveguide, cladding and the grating, where all these parameters can easily be tailored during the process of fabrication of the device [15].

3. Design of LPWG filter

3.1. LPWG band reject filter

The schematic diagrams of the nano-deep corrugated LPWGs filters are shown in Figs. 1 and 2, where the former one acts as a band rejection filter and the latter one acts as a band-pass filter. LPWG with a grating period Λ is formed along the core of a channel waveguide, where n_g, n_{ucl}, n_{ocl}, and n_{ex} are the refractive indices of the guiding layer, undercladding, overcladding, and the external medium, respectively, with $n_g > n_{ucl} = n_{ocl} > n_{ex}$, thicknesses of the guiding layer, under- and over-claddings are considered as d_g, d_{ucl} and d_{ocl} ($d_{ucl} = d_{ocl}$, in case of use of the same material in identical condition) respectively. The polymer materials considered for the guiding layer, under and overcladding layers are SU-8 2005 and NOA61, respectively. The design parameters for LPWG filter are considered as $n_g = 1.57$, $n_{ucl} = n_{ocl} = 1.55$ and $n_{ex} = 1$ with $d_g = 3.9$ μm, $d_{ucl} = d_{ocl} = 6.7$ μm. The dimension of the waveguide core with a W/T (W and T are the width and thickness of the waveguide) ratio ensures the single-mode operation of the waveguide at 1550 nm. A length of 15 mm is patterned as a nano-deep corrugated grating on middle section of a waveguide length of 30 mm. The corrugated grating parameters, like as grating period Λ, are calculated from the phase matching graphs and grating tooth height (t_d) is optimized by OptiGrating 4.2 software tool. Considering these waveguide parameters, it is investigated that the resonance wavelength strongly depends upon the grating parameters. The central task of this design ensures the coupling between fundamental guided mode to the second order cladding mode so that strong rejection bands are achieved in visible and IR wavelength regions in transmission spectra for a particular grating period and tooth height.

3.2. LPWG band pass filter

In WDM-based technology, for the separation of various wavelength channels, band pass filters are required, which can also be developed with LPWGs .The schematic diagram of LPWG band pass filter is shown in Fig. 2. The design is consisting of two corrugated LPWGs with common cladding which are connected in series with a gap introduced in the middle of the core. The core is removed in this gap. Two LPWGs have same grating period Λ and separated by gap d. The first LPWG couples light from fundamental core mode to higher order cladding modes at the specific resonance wavelength. These cladding modes propagate through the cladding region and coupled back into the second LPWG core, which has identical grating parameters. The gap distance between two core waveguides is optimized so that only specific higher order cladding modes as per the resonance wavelength of the first LPWG are coupled back to the core of the second LPWG through the common cladding eventually forming a band pass filter at the output of the second LPWG. At the same time, the discontinuity (gap) between two waveguides restricts the propagation of the forward-propagating fundamental core-mode into the core of the second waveguide.

4. Results and discussions

Once the effective mode indices for fundamental core-mode and the specific higher order cladding modes are calculated by mode solver, the resonance wavelength of the LPWG for a particular periodicity can be evaluated by use the phase matching condition, as mentioned in Eq. (1). Accordingly, the phase matching curve can be achieved for the LPWG, which describes the relation between the resonance wavelength and the grating period. These curves are shown in Fig. 3(a) and (b), which determines a particular grating period to filter out a certain wavelength from the entire transmission spectrum of the waveguide. The phase matching curves are drawn for TE_i and TM_i ($i = 1, 2$) modes of the

Please cite this article in press as: M. Sharma, S. Pal, Design and analysis of nano-deep corrugated waveguide grating-based dual-resonant filters in visible and infra-red regions, Optik - Int. J. Light Electron Opt. (2013), http://dx.doi.org/10.1016/j.ijleo.2012.10.066

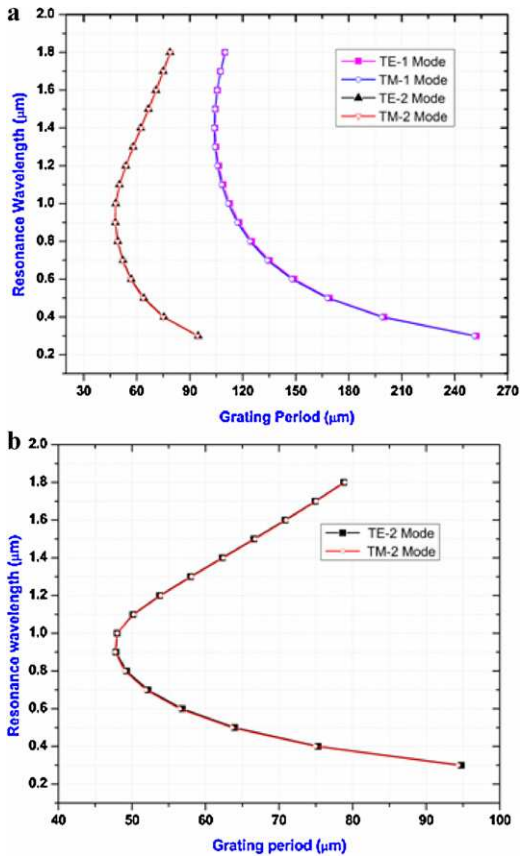

Fig. 3. Phase-matching curves for LPWGs with $d_g = 3.9\,\mu m$, $d_{u\text{-}cl} = d_{o\text{-}cl} = 6.7\,\mu m$ and $n_g = 1.57$, $n_{o\text{-}cl} = n_{u\text{-}cl} = 1.55$, $n_{ex} = 1$ (a) for various TE_i and TM_i modes (for $i = 1, 2$), (b) for showing the difference between TE_2 and TM_2 modes.

LPWG considering refractive indices of guiding (n_g), over- (n_{ocl}) and under-cladding (n_{ucl}) layers are $n_g = 1.57$, $n_{ocl} = 1.55$, $n_{ucl} = 1.55$, respectively, considering guiding layer thickness $d_g = 3.9\,\mu m$, along with a symmetrical under-cladding and over-cladding layer thickness, $d_{ocl} = d_{ucl} = 6.7\,\mu m$. A relationship among the resonance wavelength for various TE_i modes ($i = 1, 2$) with the corresponding grating pitch has been studied from this graph. It is observed that the phase matching curves for TE_i and TM_i polarizations are almost same. Fig. 3(b) displays a closer look of the phase matching graphs for the above-mentioned TE_2 and TM_2 polarization, which are also almost identical showing negligible polarization dependence.

From the phase matching graphs it is clear that the power transfer between the fundamental guided mode to first-order cladding mode at a wavelength of ~1550 nm can be achieved for a grating period of ~105 μm. Considering the above waveguide parameters, LPWG design is optimized for grating length of 15 mm with tooth height (t_d) of grating corrugation of 127 nm so that a strong rejection band (having an isolation strength of ~25.7 dB) is achieved. The resonance wavelength has been achieved at a wavelength of 1549 nm (for TE_1-mode) as shown in Fig. 4. In fact, this is the transmission spectrum (showing the band reject filter characteristics) at the output of the LPWG structure, as shown in Fig. 1. However, the transmission spectrum displays the band pass filter characteristics at the output of the LPWG structure, as shown in Fig. 2, which is also shown in Fig. 4. In this case, the design parameters of LPWG band pass filter are considered similar to that of LPWG band rejection filter ($n_g = 1.57$, $n_{ucl} = n_{ocl} = 1.55$ and $n_{ex} = 1$ with $d_g = 3.9\,\mu m$, $d_{ucl} = d_{ocl} = 6.7\,\mu m$) along with a separation gap of 500 μm between the two waveguides, as shown in Fig. 2. That is why the central wavelength of the band pass filter is achieved at the same

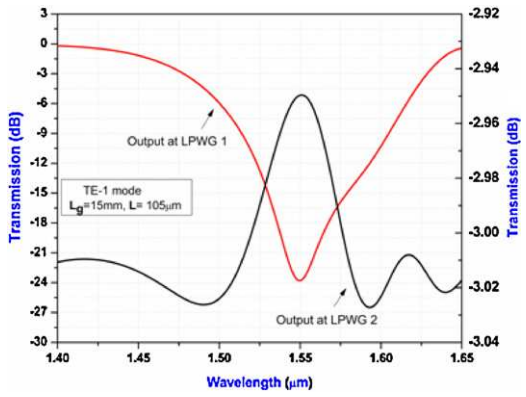

Fig. 4. Transmission and reflection spectra for TE_1 mode for a grating period of 105 μm with grating tooth-height (t_d) of 127 nm. The transmission spectra show the corresponding band-reject and band-pass filter characteristics when a broad-band signal is transmitted through the LPWG structures shown in Figs. 1 and 2, respectively.

wavelength of 1549 nm (for TE_1-mode) with only the difference of having less magnitude of reflectivity in comparison to the transmission spectrum. In fact, the fundamental core-mode couples to specific first higher order cladding mode depending on the periodicity of the first LPWG, which propagates through the cladding region and then again coupled back to core region of the second LPWG. However, the fundamental core-mode incident at the input of the first LPWG does not propagate into the second LPWG core region due to the separation gap (discontinuity in the core waveguide). These facts are responsible of showing a band pass filter characteristics at the output of second LPWG. Both the band-rejection and band-pass filter characteristics for the designed LPWGs corresponding to the same resonance wavelength are shown in Fig. 4.

The behavior of the phase-matching curve for TE_2 and TM_2 anticipates the dual resonance of the LPWG for a particular grating period. Fig. 5(a) and (b) describes the transmission spectral characteristics of the LPWG (structure as shown in Fig. 1) for a grating period of 68 micron with different tooth-height corrugation of the grating. Two distinct rejection bands are observed due to the dual-resonance nature of the designed LPWG having one resonance wavelength at around 1532 nm (infra-red communication region) and the other resonance wavelength at around 454 nm (visible blue). Therefore, the design is further modified after optimizing the grating tooth-height (t_d) in order to achieve strong isolation dips (to optimize the value of coupling coefficient of the LPWG for the desired condition) at both visible and IR wavelength regions simultaneously and separately. For the grating period of 68 μm, a strong rejection band having the strength of ~25 dB is achieved at a resonance wavelength of 454 nm (visible blue region) along with a weaker resonance dip at around 1532 nm when the tooth-height of grating corrugation (t_d) is optimized to a value of 195 nm. Considering the same grating period, when the grating tooth-height (t_d) is optimized to a value of 913 nm, a strong rejection band of strength of ~23 dB is achieved at a wavelength of 1532 nm (infra-red communication region) for TE polarization as shown in Fig. 5(a). In the next stage, the grating design is modified so that these two band rejection filters can be achieved simultaneously with almost similar isolation strength with a grating tooth height of 725 nm, considering the same grating period. The transmission spectral characteristics for this LPWG are shown in Fig. 5(b), where two resonance wavelengths are achieved at 454 nm (~18 dB) and 1534 nm (~15 dB). The length of the grating has been considered as 15 mm in the design. The summary of simulation results for the LPWG (designed for different condition) is shown in Table 1, which clearly

Please cite this article in press as: M. Sharma, S. Pal, Design and analysis of nano-deep corrugated waveguide grating-based dual-resonant filters in visible and infra-red regions, Optik - Int. J. Light Electron Opt. (2013), http://dx.doi.org/10.1016/j.ijleo.2012.10.066

Table 1
Summary of the simulation results for a polymeric LPWG having grating length of 15 mm at different conditions.

S. no.	Coupling modes	Grating period (μm)	Grating tooth height (nm)	Resonance wavelength (nm)	Transmission (dB)
1.	TE-1	105	127	1549	−25.7
2.	TE-2	68	195	458	−24.46
3.	TE-2	68	913	1532	−23.03
	TM-2	68	900	1530	−43.72
4.	TE-2	68	725	454	−17.8
				1534	−15.1

shows that the proper choice of grating parameters of the LPWG would lead to develop strong rejection filters both at visible as well as IR wavelength regions. This property can be exploited for various sensing applications for a wider dynamic range of measurement in addition to its utilization for visible and infra-red region sensing applications simultaneously or separately.

The transmission spectra of LPWGs are also analyzed for different grating lengths (L_g), say, for a length of 3 mm and 10 mm. This has been studied for coupling between fundamental core-mode and first order cladding mode of LPWG having periodicity of 105 μm, for TE polarization. In case of a grating length of 3 mm, the resonance wavelength is achieved at ∼1555 nm with isolation strength of ∼48 dB when the tooth height of grating corrugation is optimized to 128 nm. However, keeping other parameters fixed, for grating length of 10 mm, the resonance is achieved at the same wavelength with maximum possible isolation strength of ∼36 dB for a relatively less value of grating tooth height of 115 nm. In next stage simulation, a similar approach is considered for coupling of fundamental core-mode to the second-order cladding-mode for a grating period of 68 μm. Optimized grating tooth-heights of 510 nm and 742 nm are found, for a grating length of 3 mm, when the resonance wavelengths are achieved at 1533 nm (∼38 dB) and 459 nm (∼35 dB), respectively. For grating length of 10 mm, the tooth height of 472 nm is optimized for resonance wavelength of 459 nm with isolation dip strength of ∼37 dB. The simulation results for different grating periods are showing that the resonance wavelength strongly depends upon the grating tooth height, which is primarily for the optimized value of coupling coefficient of the LPWG depending on grating length.

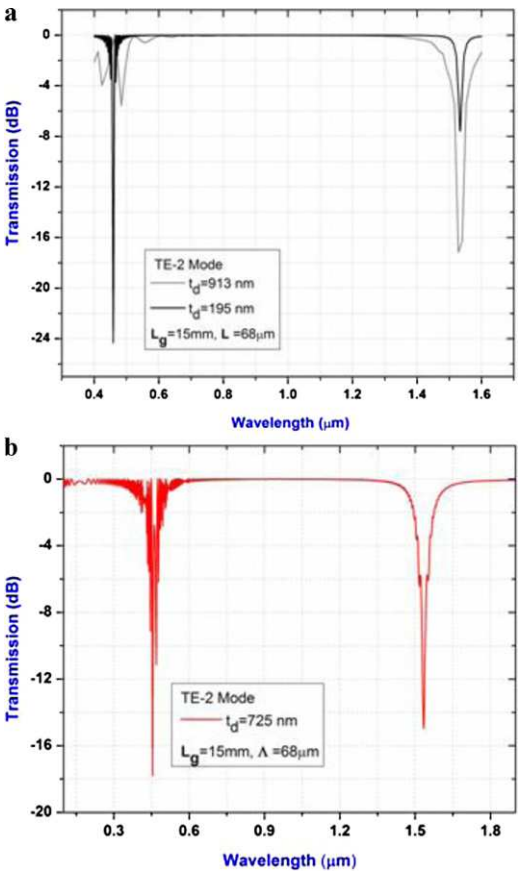

Fig. 5. (a) Transmission spectra of LPWG band reject filter and dependence of its resonance wavelength on the grating tooth-height (t_d). For an LPWG, with a grating period of 68 μm having grating tooth height of 913 nm results in the resonance wavelength in IR region. The same LPWG, for t_d = 195 nm, results in a resonance wavelength in the visible-blue region. (b) Transmission spectrum for LPWG having resonance wavelength both in the visible-blue as well as in the infra-red regions with an optimized grating tooth height of 725 nm for a grating period of 68 μm.

The temperature-effects on the designed polymer-based LPWG are also analyzed, as the thermo-optic coefficients of these materials are relatively high. The values of refractive indices of different layers of the device will change along with a slight change in the periodicity of the grating (due to thermal expansion coefficient), which results in shift in the resonance wavelength of the LPWG. In this study, the phase-matching curves are drawn considering the coupling of fundamental core-mode with the second-order cladding-mode at the different temperatures, say, for 0 °C, 25 °C, 50 °C and 75 °C. The values of thermo-optic coefficients (TOC) for SU8 polymer has been considered as -1.75×10^{-4}/°C [16] and that for NOA61 polymer as -1.98×10^{-4}/°C according to the data sheet. TOCs for both of these polymers are found to be negative, which may result in relatively less stress within the interface of the layers. The expansion of the grating periodicity of LPWG is ignored in this study, as the values of thermal expansion coefficients are more than one order less compared to their TOC values. The plots of phase matching graphs corresponding to different temperatures are shown in Fig. 6. As the temperature increases from 0 °C to 75 °C, both the resonance wavelengths (due to dual-resonance property) are found to be shifted. A significant amount of red-shift for the longer wavelength resonance (infra-red region) and a relatively less

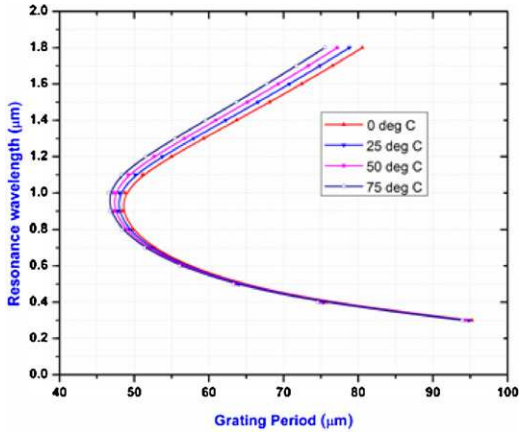

Fig. 6. Variation of the phase matching graph of the LPWG designed for TE_2 mode for different temperatures.

Please cite this article in press as: M. Sharma, S. Pal, Design and analysis of nano-deep corrugated waveguide grating-based dual-resonant filters in visible and infra-red regions, Optik - Int. J. Light Electron Opt. (2013), http://dx.doi.org/10.1016/j.ijleo.2012.10.066

amount of blue-shift for the shorter wavelength resonance (visible blue region) are observed for the increase of temperature. This temperature-effect on resonance wavelength clearly shows the thermal tunability of the LPWG filter and this property can be utilized for multi-parameter sensing and temperature compensated sensing applications.

5. Conclusions

Polymer nano-deep corrugated LPWG-based band reject filter and band pass filter are theoretically analyzed. A grating period of 68 μm is considered on a symmetrical waveguide based on SU-8 and NOA-61 polymer materials in order to achieve two rejection bands at visible-blue as well as at infra-red wavelength regions. The simulation results explain the variation of the resonance wavelength with the change in nano-deep grating tooth height. The optimized grating tooth height of 913 nm, 195 nm and 725 nm provides rejection bands both in IR and visible wavelength regions. This type of LPWG filters has potential for visible and infra-red wavelength sensing applications separately and simultaneously.

Acknowledgments

Authors would like to thank the Director, CSIR-CEERI, Pilani, for his encouragement, and to all members of the Optoelectronic Devices Group for their help and cooperation.

References

[1] A.M. Vengsarkar, P.J. Lemaire, J.B. Judkins, V. Bhatia, T. Erdogan, J.E. Sipe, Long-period fiber gratings as band rejection filters, J. Lightwave Technol. 14 (1996) 58–65.
[2] V. Rastogi, K.S. Chiang, Long-period gratings in planar optical waveguides, Appl. Opt. 41 (2002) 6351–6355.
[3] H.C. Tsoi, W.H. Wong, B.E.Y. Pun, Polymeric long-period waveguide gratings, IEEE Photon. Technol. Lett. 15 (2003) 721–724.
[4] Q. Liu, K.S. Chiang, K.P. Lor, Long period grating in polymer ridge waveguides, Opt. Express 13 (2005) 1150–1160.
[5] Y.M. Chu, K.S. Chiang, Q. Liu, Widely tunable optical band pass filter by use of polymer long-period waveguide gratings, Appl. Opt. 45 (2006) 2755–2760.
[6] M.S. Kwon, S.Y. Shin, Tunable notch filter using a thermo-optic long-period grating, J. Lightwave Technol. 22 (2004) 1968–1975.
[7] B.D. Choudhury, S. Pal, B.R. Singh, Optimal design of silica-based temperature-insensitive long-period waveguide gratings for realization of athermal refractive-index sensor, Sens. Actuators A 141 (2008) 328–333.
[8] K.S. Chiang, C.K. Chow, H.P. Chan, Q. Liu, K.P. Lor, Widely tunable polymer long-period waveguide grating with polarization-insensitive resonance wavelength, Electron. Lett. 40 (2004) 422–423.
[9] Y. Bai, K.S. Chiang, Analysis and design of long-period waveguide-grating couplers, J. Lightwave Technol. 23 (2005) 4363–4373.
[10] Y. Bai, Q. Liu, K.P. Lor, K.S. Chiang, Widely tunable long-period waveguide grating couplers, Opt. Express 14 (2006) 12644–12654.
[11] Q. Liu, K.S. Chiang, K.P. Lor, Dual resonance in a long period waveguide grating, Appl. Phys. B Laser Optics 86 (2007) 147–150.
[12] R. Singhal, M.N. Satyanarayan, S. Pal, Effect of residual resist on performance of single-mode 1 × 4 optical splitter in photosensitive polymer, Fiber Integr. Opt. 29 (2010) 480–490.
[13] A. Yariv, Optical Electronics in Modern Communications, Oxford University Press, New York, 1997.
[14] S. Pal, B.R. Singh, Analysis and design of corrugated long period gratings in silica on silicon planar waveguide, IEEE J. Lightwave Technol. 25 (2007) 2260–2267.
[15] S. Pal, A. Chauhan, P. Kumar, M. Singh, N. Pradhan, M.K. Sharma, K. Singh, C. Dhanvantri, Realization of corrugated long-period gratings in silica-on silicon-based channel waveguide, IEEE Photon. Technol. Lett. 21 (2009) 1490–1492.
[16] H.Y. Tang, W.H. Wong, E.Y.B. Pun, Long period polymer waveguide grating devices with positive temperature sensitivity, Appl. Phys. B 79 (2004) 95–98.

Please cite this article in press as: M. Sharma, S. Pal, Design and analysis of nano-deep corrugated waveguide grating-based dual-resonant filters in visible and infra-red regions, Optik - Int. J. Light Electron Opt. (2013), http://dx.doi.org/10.1016/j.ijleo.2012.10.066